Improved High-Frequency Planar Transformer for Line Level Control (LLC) Resonant Converters

Magnetic Instruments

Improved Structure of Integrated Magnetics for High Frequency LLC Resonant Converters (Revised Sep 2013)

Wayne. Water[1*] , and Junwei. Lu[1**]

[1] *School of Engineering, Griffith University, Nathan, QLD 4111, Australia*

** Student Member, IEEE*

*** Senior Member, IEEE*

Abstract— In this letter, an improved structure of High Frequency (HF) magnetic integrated planar transformer is proposed and the prototype transformer is demonstrated. In comparison to conventional planar integrated magnetics; the improved structure has a better ability on leakage inductance adjustment. Also; instead of using expensive Printed Circuit Board (PCB) windings on the primary side, multi-strand Litz wires are used for the design. The transformer is fabricated with two common EE shape magnetic cores along with magnetic insertions placed between the primary and secondary windings (outside the main core). To analyze the proposed transformer, the numerical 3-D Finite Element Method (FEM) technique is employed to investigate the eddy current losses and the adjustment of the leakage inductance.

Index Terms—Magnetic instruments, finite element methods, integrated circuit fabrication, transformers

I. INTRODUCTION

There are several different magnetically integrated transformers have been designed for LLC converters; however, efforts are still needed to further reduce the transformer volume while maintaining the controllability of the leakage inductance (L_s). The simplest structure of an LLC transformer is by designing an extra core on top of the transformer [Hangseok 2007]. [Stegen 2011, Yanjun 2007, Yang 2002] have a similar structure but L_s is designed on the side of the transformer. These two structures are very reliable and effective with the design process as L_s and L_p have their own flux path.

A more cost-effective design has been introduced by [Chen 2001], where the magnetic integration is achieved by introducing the magnetic insertion inside the transformer between primary and secondary windings. This design reduces the volume of integrated magnetics compared to the other designs, as there are no protruding magnetic pieces. However, the disadvantage of this structure is that the adjustment of L_s mainly relies on the physical dimensions of the magnetic piece; when assuming winding distances and dimensions of magnetic components are fixed. PCB windings utilized by [Chen 2001] have a higher manufacturing cost and increase the complexity of the transformer fabrication process when compared to utilizing Litz wire. Therefore, an improved structure of the magnetic integrated transformer is introduced in this letter which has advantages of low profile, controllability of the L_s, high efficiency and low cost in comparison with above structures.

II. TRANSFORMER DESIGN AND FABRICATION

A. Proposed Structure of Integrated LLC Transformer

Fig. 1 shows the difference between the flux directions of the Magnetic Insertion in Parallel (MIP) structure [Chen 2001] and the proposed Magnetic Insertion placed Orthogonally (MIO) transformer structure. The major improvement to the structure of MIP is the position of the magnetic insertion, which is placed outside of the transformer. Two major benefits are obtained from doing this; firstly, the current distribution in the windings becomes more evenly distributed, and secondly; there is flexibility in the adjustment of L_s.

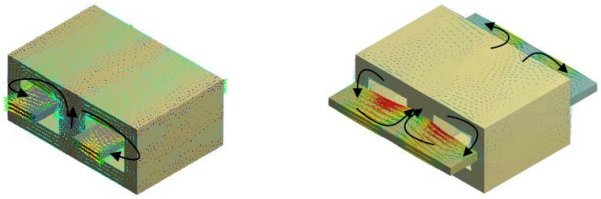

(a) MIP [Chen 2001] (b) MIO [Proposed]

Fig. 1. The comparison of flux direction

The structure of the prototype transformer is shown in Fig. 2, where EE cores are used as the transformer core with primary and secondary windings on each end of the window. The magnetic insertion is placed horizontally between the primary and secondary windings, where the primary is fabricated with 14 strands of twisted Litz wire and the secondary is fabricated with cut copper sheets.

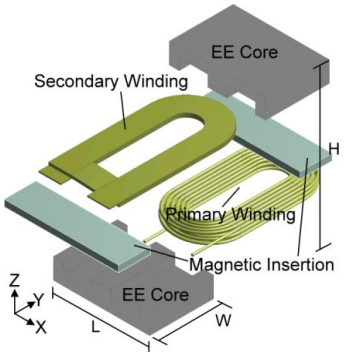

Fig. 2. The explorered view of the introduced LLC transformer

Corresponding author: W. Water (wayne_water@hotmail.com)

B. Transformer Requirements and Fabrication

Two prototype transformers were built with the same specifications but using different EE core sizes and conductor dimensions. Both transformers were required to have a power rating of 1.08 kW, output voltage of 36 V, nominal input voltage of 216 V (voltage ratio of 18:3), resonant frequency at 90 kHz, and an inductance ratio of 5, with the magnetizing inductance (L_p) at 175 μH and the L_s at 33 μH respectively. Both prototypes were required to have an operating temperature between 60 and 80 degrees Celsius. The detailed dimensions of prototype I is shown in in Fig. 3, where the dimensions of the EE core is 38/25/16; $L/W/H$ respectively in mm. Prototype II utilized an EE core of dimensions 43/28/19; $L/W/H$ respectively in mm. Prototype images of I is shown in Fig. 4(a), and II is shown in Fig. 4 (b).

The magnetic materials chosen for the design are NiZn and MnZn for prototype I and prototype II respectively; saturated flux densities are 430 mT and 510 mT respectively for both materials at room temperature. The relative permeability of the magnetic materials as well as the air-gap and insertion gap is tabulated in Table 1. Furthermore, for primary windings on prototype I, each strand has the diameter of 0.25 mm; whereas the secondary is with the dimension of 0.25 X 8.8 mm (*LxW*). In comparison, primary windings on prototype II, each strand has the diameter of 0.321 mm; whereas the secondary is with the dimension of 0.4 X 10 mm (*LxW*).

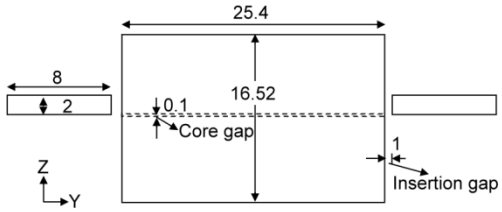

(a) Side view

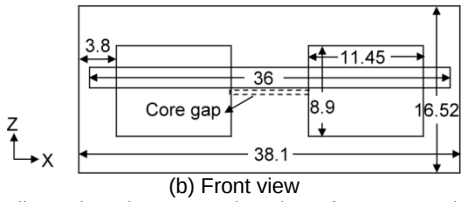

(b) Front view

Fig. 3. The dimensioned cross-section view of prototype I (unit: mm)

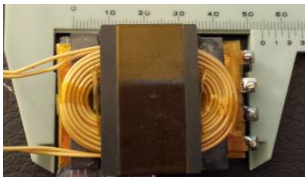

(a) Prototype I

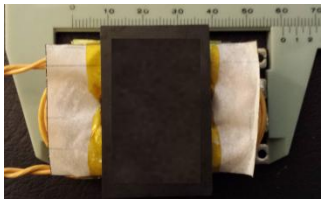

(b) Prototype II

Fig. 4. Transformer protoypes

Table 1. The magnetic characteristic and gapping information

	μ_r	Core gap	Insertion gap
Prototype I	120	0.1 mm	1 mm
Prototype II	2400	0.3 mm	2 mm

III. INDUCTANCE ANALYSIS

The FEM in conjunction with the *Energy Method* was chosen for the inductance computation due to a higher accuracy [Thondapu 2012]. Table 2 shows the inductance requirements and comparisons between the MIP and MIO structure (refer to Fig. 1). The maximum L_s can be obtained by maximizing the winding distance for the selected core size is 12.99 μH; in order to fulfill the requirement, either MIP or MIO structure needs to be implemented. Both EE cores for MIP and MIO will have the same inductance characteristics prior to the addition of an insertion. As can be seen, the L_p values for the MIP structure can be adjusted to fit the requirement with ease, but L_s cannot be varied easily without increasing the physical dimensions of the insertion. The MIO structure on the other hand has the ease of fulfilling the L_p requirement like the MIP structure, but also the L_s requirement by simply adjusting the insertion gap. Adjusting the distance of the insertion gap benefits both the variability of L_p and L_s, as the insertion is magnetically coupled to the transformer core. This reduces the manufacturing costs as the same transformer can be utilized for different requirements without modifying the dimensions of the magnetic materials.

Table 2. The Inductance comparison between different configurations of magnetic insertion arrangements

Structure	Insertion Configuration:	L_p (μH)	L_s (μH)
	Requirement	**175**	**33**
	No insertion	175.67	12.99
MIP	Inside the core	175.81	29.93
MIP	Length increased to 50.4 mm	175.84	34.96
MIO	1 mm insertion gap	174.04	34.82
MIO	No insertion gap	184.08	98.70

IV. 3-D SIMULATION RESULTS

To evaluate both the transformers performance, a commercial electromagnetic software package; *ANSYS Mechanical 13.0* was used to conduct the analysis.

A. Magnetic Field Distribution

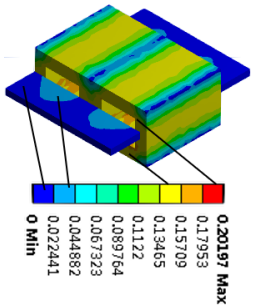

(a) OC

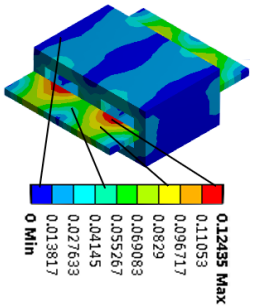

(b) SC

Fig. 5. Magnetic flux density of prototype I (OC: open circuit condition, SC: short cirucit condition)

Only prototype I result is shown as both prototypes displayed a similar flux distribution (Fig. 5). In Fig. 5, the result demonstrates how leakage inductance is adjusted with the use of the magnetic insertion. The amount of energy stored in

the air core is limited, and cannot be increased easily unless the distance between windings is further increased. However, with the use of the magnetic insertion, the leakage inductance can be adjusted freely by controlling the insertion gap without increasing the transformer volume. Under the open circuit condition (light-load condition), the flux density of prototype II is 11.94% lower than to prototype I. This satisfies Faraday's law, that the magnetic flux flows in the core is inversely proportional to the core area. The maximum flux densities for both prototypes I and II at full-load (short circuit) and light-load conditions are in the linear region of operation.

B. Analysis of Current Density

The 3-D result of the current distribution is shown in Fig. 6. Unexpectedly, the peak current density in prototype II is 25.53% higher than in prototype I under short circuit condition. The conductor dimension of the prototype II is designed at a greater size compared to the prototype I, however, it was demonstrated by both the simulation result and the measurements that the conductor dimension should be always smaller than double of the skin depth [Wayne 2012]. The peak current density of the prototype II is higher than prototype I due to the skin effect and the proximity effect. The current distribution in HF can be described as the relationship to the AC resistance [Ferreira 1994]:

$$R_{ac} = \frac{R_{dc}\cdot\xi}{2}\cdot\frac{\sinh\xi+\sin\xi}{\cosh\xi-\cos\xi} + (2m-1)^2\cdot\frac{\sinh\xi+\sin\xi}{\cosh\xi-\cos\xi} \quad (1)$$

where ξ is defined as:

$$\xi = \frac{\sqrt{\pi}}{2}\cdot\frac{d}{\delta} \quad (2)$$

(d: conductor diameter, δ: skin depth)

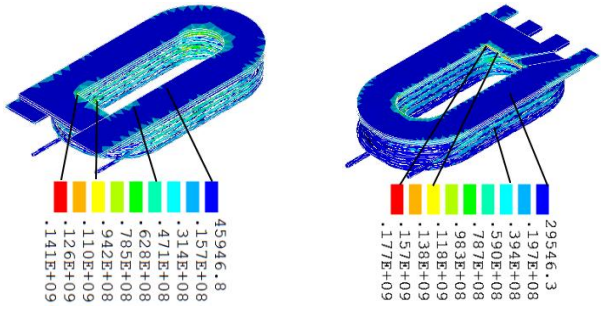

(a) Prototype I (b) Prototype II

Fig. 6. Eddy current simulation under short circuit condition.

As both prototype cores utilize high efficiency Ferrite material, copper losses in the core and the insertion are very small which can almost be neglected (Table 3). Prototype II has a 16.38% higher full load winding losses compared to prototype I (prototype I - 11.8515 W, prototype II - 13.793 W); where the full load winding losses is the sum of the winding losses under both open circuit condition and short circuit condition. Based on both the eddy current and winding loss simulation results, the following design principles are made and should be followed to minimize the AC losses: (1) the dimension of conductors needs to be smaller than the skin depth; (2) the winding layers and transformer winding turns must be minimized; (3) the core gap must be less than 3 mm to minimize the fringing effect; and (4) both primary and secondary windings should be placed away from the core gap, to minimize the induced eddy currents from the core gap.

Table 3. Simulation result power loss of prototype I and II at 90 kHz
OC: open circuit condition; SC: short circuit condition (P_I: prototype I, P_{II}: prototype II)

(Unit : W)		Primary	Secondary	Core	Insertion
OC	P_I	1.0435	0.8316	7.46E-09	3.00E-12
	P_{II}	1.9277	0.6097	6.67E-03	2.03E-06
SC	P_I	4.1286	5.8477	7.91E-11	3.31E-11
	P_{II}	5.3437	5.9117	8.32E-05	3.62E-05

V. EXPERIMENT RESULTS

The transformer has been tested with a 1.1kW resistive element and did not exceed the working temperature. The *HAMEG HM8118 LCR Meter* (20Hz to 200 kHz) was utilized to measure the transformer parameters, with the measurement results shown in Table 4. R_p, R_s and C_p denote core loss resistance, winding resistance and intra-winding capacitance respectively. Apart from L_p, all parameters are frequency dependent. R_p and R_s power loss can be calculated through the use of Ohm's law at a specific frequency point;

$$P \propto {I_{ac}}^2 \cdot R \quad (3)$$

where I_{ac} is the current in AC mode. For the power losses calculation of the introduced prototype transformers, $I_{ac} = 5A$ if R_s is utilized, and $I_{ac} = 5.18\times10^{-3}A$ and $2.42\times10^{-2}A$ for prototype I and prototype II respectively if R_p is utilized. Please note that the core losses stated in Table 3 is the copper losses of the core; in which distributes partial losses of the overall core losses calculated above with the use of (3).

R_p was found to be higher in prototype I due to the lower resistivity of the core when compared to prototype II; also, the significant difference of R_p at 90 kHz is because of the non-linear characteristic of the magnetic material between prototypes. R_s was found to be lower in prototype I due to lower eddy current effects, fringing effects and proximity effects. C_p was found to be slightly smaller in prototype II, which can be attribute to a greater distance between the primary and the secondary windings compared to prototype I.

Table 4. The measurement results of the prototypes under different frequencies (P_I: prototype I, P_{II}: prototype II)

		L_p (μH)	R_p (kΩ)	L_s (μH)	R_s (Ω)	C_p (pF)
Requirement		175	N/A	33	N/A	N/A
10 kHz	P_I:	173.64	1.164	34.26	0.369	29.775
	P_{II}:	176.17	1.24	35.72	0.439	29.56
90 kHz	P_I:	173.25	38.7	32.797	0.968	30.62
	P_{II}:	174.95	8.31	33.504	1.132	30.5
200 kHz	P_I:	174.43	93.7	32.422	2.0541	36.744
	P_{II}:	175.58	76.749	32.796	2.1025	36.312

The signal generator and the oscilloscope were used to obtain the waveform measurements of prototype transformers directly; results are shown in Fig. 7, where the top waveform (1) is the input voltage and the bottom waveform (2) is the output voltage. Due to the integration of the leakage inductance, a voltage pulse on the rising edge of the output can be observed. Prototype I has a higher voltage pulse than prototype II, as prototype II has a greater parasitic-capacitance (self-capacitance), in which the capacitance regulates the voltage pulse. Furthermore, self-resonant frequency were obtained by connecting a 1 kΩ resistor to the transformer input, and then monitor the frequency where the transformer has the maximum and minimum voltage distribution. Series self-resonant frequencies are 10.28 MHz and 9.44 MHz, and parallel self-resonant frequencies are 16.55 MHz and 14.75 MHz respectively for prototype I and prototype II. Since the operating frequency requirement is at 90 kHz, the prototype transformers are guaranteed to operate safely, as the requirement frequency is well below the self-resonant frequencies.

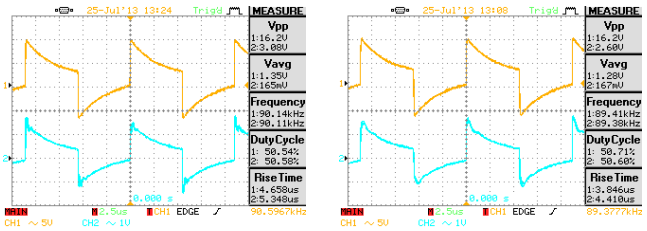

(a) Prototype I (b) Prototype II

Fig. 7. Square wave test of prototypes at 90 kHz

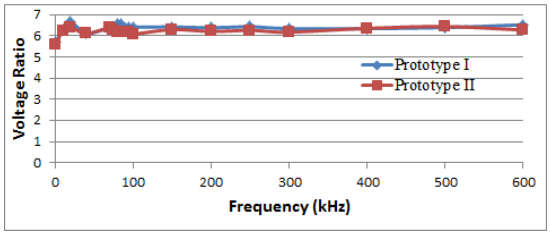

Fig. 8. Voltage/turn ratio of HF planar transformers

The ideal voltage ratio should be the same as the transformer turn ratio of 6:1, but from the measurement results in Fig. 8, the voltage ratio maintains an average value of between 6.2 and 6.5 thought the frequency range. This increase of the voltage ratio can be attributed to the existence of the air-core section of L_s. Because of the unique structure of the introduced transformer, If the voltage is measured without the load (open circuit case), only air-core leakage inductance in primary is taking the effect. This also makes the introduced structure more advantageous (higher efficiency) at no-load condition compared to the top-up or add-on structure in other references [Hangseok 2007, Stegen 2011, Yanjun 2007, Yang 2002]. From Table 5; the simulation of leakage inductance without the insertion was found to be 12.99 μH. When the voltage divider principal is applied, the voltage delivered to L_p is reduced by a factor of 0.069, which results in a voltage ratio increase to 6.445:1. This voltage ratio increase agrees with the measurement results.

VI. DISCUSSION

The winding resistance result shown in Fig. 9 verifies the accuracy of simulation results to measurements. There is a small variation of 0.11 – 0.18 Ω between the simulation results and measurements. The difference can mainly be attributed to the wire used to short-circuit the secondary side, in which the wire resistance is being amplified in the step-down transformer when coupled to the primary side. This phenomenon becomes more apparent as the frequency increases. As manufacturing techniques are imperfect; issues such as the soldered connection points diverge the measured results from the simulated model. This consideration of termination effects should be undertaken as further work on simulation models. Comparing the simulations to the measurements, some conclusions can be made. The conductor thickness should stay within the skin depth in order to minimize winding losses. A larger core dimension will reduce core losses, with a maximum efficiency where the core losses are equal to the winding losses.

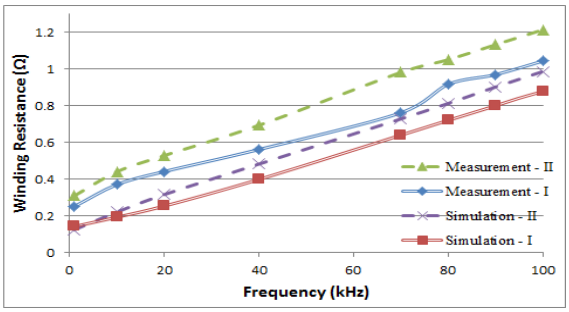

Fig. 9. Winding resistance simulation result versus measurements

REFERENCES

Chen R, Stridom JT and Wyk JDV (2001), "Design of planar integrated passive module for zero-voltage switched asymmetrical half bridge PWM converter," *36th Annu. Industry Application. Conf.*, vol. 4, pp. 2232-2237.

Hangseok C (2007), "Analysis and Design of LLC Resonant Converter with Integrated Transformer," in *APEC. 22nd Annu. Applied Power Electron. Conf.*, pp. 1630-1635.

Stegen S, and Lu J (2011), "Structure Comparison of High-Frequency Planar Power Integrated Magnetic Circuits," *IEEE Trans. on Magnetics*, Vol. 47, No. 10, pp. 4425-4428.

Thondapu SR, Borage MB, Wanmode YD and Shrivastava P (2012), "Improved Expression for Estimation of Leakage Inductance in E Core Transformer Using Energy Method", *Advances in Power Electronics*, vol. 2012, Article ID 635715.

Yang B, Chen R and Lee FC (2002), "Integrated magnetic for LLC resonant converter," in *APEC. 17th Annu. Applied Power Electron. Conf.*, vol. 1, pp. 346-351.

Yanjun Z, Dehong X, Kazuaki M and Kiyoaki S, "1MHz-1kW LLC Resonant Converter with Integrated Magnetics (2007)," in *APEC. 22nd Annu. Applied Power Electron. Conf.*, pp. 955-961.

Water W and Lu J (2012), "Eddy current and Structure Optimization of High Frequency Coaxial Transformers Using the Numerical Computation Method," in *ICEF. 6th Annu. Electromagnetic Field Problems and Applications Conf.*, pp. 1-4.

Ferreira JA (1994), "Improved Analytical Modeling of Conductive Losses in Magnetic Components", *IEEE Trans. on Power Electronics*, vol. 9, no. 1, pp. 127-131.